



Logarithmic and Power Law Input-Output Relations in Sensory Systems with Fold-Change Detection

Miri Adler, Avi Mayo, Uri Alon*

Department of Molecular Cell Biology, Weizmann Institute of Science, Rehovot, Israel

Abstract

Two central biophysical laws describe sensory responses to input signals. One is a logarithmic relationship between input and output, and the other is a power law relationship. These laws are sometimes called the Weber-Fechner law and the Stevens power law, respectively. The two laws are found in a wide variety of human sensory systems including hearing, vision, taste, and weight perception; they also occur in the responses of cells to stimuli. However the mechanistic origin of these laws is not fully understood. To address this, we consider a class of biological circuits exhibiting a property called fold-change detection (FCD). In these circuits the response dynamics depend only on the relative change in input signal and not its absolute level, a property which applies to many physiological and cellular sensory systems. We show analytically that by changing a single parameter in the FCD circuits, both logarithmic and power-law relationships emerge; these laws are modified versions of the Weber-Fechner and Stevens laws. The parameter that determines which law is found is the steepness (effective Hill coefficient) of the effect of the internal variable on the output. This finding applies to major circuit architectures found in biological systems, including the incoherent feed-forward loop and nonlinear integral feedback loops. Therefore, if one measures the response to different fold changes in input signal and observes a logarithmic or power law, the present theory can be used to rule out certain FCD mechanisms, and to predict their cooperativity parameter. We demonstrate this approach using data from eukaryotic chemotaxis signaling.

Citation: Adler M, Mayo A, Alon U (2014) Logarithmic and Power Law Input-Output Relations in Sensory Systems with Fold-Change Detection. *PLoS Comput Biol* 10(8): e1003781. doi:10.1371/journal.pcbi.1003781

Editor: Jorg Stelling, ETH Zurich, Switzerland

Received: January 29, 2014; **Accepted:** June 24, 2014; **Published:** August 14, 2014

Copyright: © 2014 Adler et al. This is an open-access article distributed under the terms of the Creative Commons Attribution License, which permits unrestricted use, distribution, and reproduction in any medium, provided the original author and source are credited.

Funding: We would like to acknowledge support for this work from the Israel Science Foundations and the European Research Council under the European Union's Seventh Framework Programme (FP7/2007-2013)/ERC Grant agreement n° 249919. Uri Alon is the incumbent of the Abisch-Frenkel Professorial Chair. The funders had no role in study design, data collection and analysis, decision to publish, or preparation of the manuscript.

Competing Interests: The authors have declared that no competing interests exist.

* Email: uri.alon@weizmann.ac.il

Introduction

Biological sensory systems have been quantitatively studied for over 150 years. In many sensory systems, the response to a step increase in signal rises, reaches a peak response, and then falls, adapting back to a baseline level, z_{st} (Fig. 1a upper panel). Consider a step increase in input signal from I_0 to I_1 , such that the relative change is $R_I \equiv \frac{\Delta I}{I} = \frac{I_1 - I_0}{I_0}$. There are two commonly observed forms for the input-output relationship in sensory systems: logarithmic and power law. In the logarithmic case, the relative peak response of the system $R_z \equiv \frac{\Delta z}{z} = \frac{z_{\max} - z_{st}}{z_{st}}$ is proportional not to the input level but to its logarithm $R_z \sim \log R_I$. A logarithmic scale of z versus I , namely $\Delta z = \log I$, is often called the Weber-Fechner law [1], and is related but distinct from the present definition $\frac{\Delta z}{z} = \log \frac{\Delta I}{I}$. In the case of a power-law relationship, the maximal response is proportional to a power of the input $R_z \sim R_I^\beta$ (Fig. 1a lower panel) [2]. In physiology this is known as the Stevens power law; the power law exponent β varies between sensory systems, and ranges between $\beta \approx 0.3 - 3.5$ [2]. For example the human perception of brightness, apparent length and electrical shock display exponents $\beta = 0.33, 1.1, 3.5$ respectively.

Both logarithmic and power-law descriptions are empirical; when valid, they are typically found to be quite accurate over a

range of a few decades of input signal. For example, both laws emerge in visual threshold estimation experiments [3]. In that study, the logarithmic law was found to describe the response to strong signals and the power-law to weak ones. However the mechanistic origins of these laws, and the mechanistic parameters that lead to one law or the other, are currently unclear. Theoretical studies have suggested that these laws can be derived from optimization criteria for information processing [4,5], such as accounting for scale invariance of input signals [6]. Both laws can be found in models that describe sensory systems as excitable media [7]. Other studies attempt to relate these laws to properties of specific neuronal circuits [8,9]. Here we seek a simple and general model of sensory systems which can clarify which mechanistic parameters might explain the origin of the two laws in sensory systems.

To address the input-output dependence of biological sensory systems, we use a recently proposed class of circuit models that show a property known as fold-change detection [10,11]. Fold change detection (FCD) means that, for a wide range of input signals, the output depends only on the relative changes in input; identical relative changes in input result in identical output dynamics, including response amplitude and timing (Fig. 1b). Thus, a step in input from level 1 to level 2 yields exactly the same temporal output curve as a step from 2 to 4, because both steps show a 2-fold change. FCD has been shown to occur in bacterial chemotaxis, first theoretically [10,11] and then by means of

Author Summary

One of the first measurements an experimentalist makes to understand a sensory system is to explore the relation between input signal and the systems response amplitude. Here, we show using mathematical models that this measurement can give important clues about the possible mechanism of sensing. We use models that incorporate the nearly-universal features of sensory systems, including hearing and vision, and the sensing pathways of individual cells. These nearly-universal features include exact adaptation—the ability to ignore prolonged input stimuli and return to basal activity, and fold-change detection—response to relative changes in input, not absolute changes. Together with information on the input-output relationship—e.g. is it a logarithmic or a power law relationship—we show that these conditions provide enough constraints to allow the researcher to reject certain circuit designs; it also predicts, if one assumes a given design, one of its key parameters. This study can thus help unify our understanding of sensory systems, and help pinpoint the possible biological circuits based on physiological measurements.

dynamical experiments [12,13]. FCD is thought to also occur in human sensory systems including vision and hearing [11], as well as in cellular sensory pathways [14–17].

FCD can be implemented by commonly occurring gene regulation circuits, such as the network motif known as the incoherent feed-forward loop (I1-FFL) [10], as well as certain types of nonlinear integral feedback loops (NLIFL) [11]. Recently, the response of an FCD circuit to multiple simultaneous inputs was theoretically studied [18]. Mechanistically, FCD is based on an internal variable that stores information about the past signals, and normalizes the output signal accordingly. We find here, using analytical solutions, that simple fold-change detection circuits can show either logarithmic or power law behavior. The type of law,

and the power-law exponent β , depend primarily on a single parameter: the steepness (effective Hill coefficient) of the effect of the internal variable on the output.

Results

Analytical solution for the dynamics of the I1-FFL circuit in its FCD regime

We begin with a common gene regulation circuit [19] that can show FCD, the incoherent type 1 feed-forward loop (I1-FFL) [10]. In transcription networks, this circuit is made of an activator that regulates a gene and also the repressor of that gene. More generally, we can consider an input X that activates the output Z , and also activates an internal variable Y that represses Z (Fig. 2). We study a model (Eq. 1, 2) for the I1-FFL with AND logic (that is, where X and Y act multiplicatively to regulate Z), which includes ordinary differential equations for the dynamics of the internal variable Y and the output Z [20–22]. We use standard biochemical functions to describe this system [23].

$$\dot{Y} = \beta_y f(X) - \alpha_y Y \quad (1)$$

$$\dot{Z} = \beta_z g(X) \frac{K_{yz}^n}{K_{yz}^n + Y^n} - \alpha_z Z \quad (2)$$

The production rate of Y is governed by the input X according to a general input function $f(X)$ (in cases where X is a transcription factor, X denotes the active state). The maximal production rate of Y is β_y . The repressor Y is removed (dilution+degradation) at rate α_y (Eq. 1). We assume here that saturating signal of Y is present, so that all of Y is in its active form. The product Z which is repressed by Y and activated by X is produced at a rate that is a function of both X and Y , denoted $G(X, Y)$. An experimental survey of *E. coli* input functions suggested that many are well described by separation of variables: the two-dimensional input function

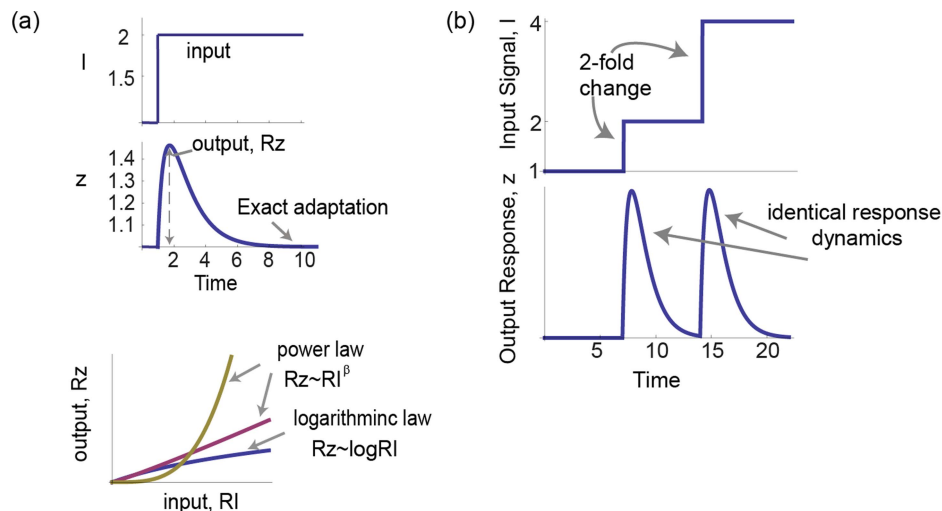


Figure 1. Input/output relationships of sensory systems can be described by a logarithmic law or a power law. a) In many sensory systems the dynamical response to a step increase in input signal, I , is a transient increase of output Z followed by adaptation to a lower steady state. The relative maximal response is $R_z \equiv \frac{z_{\max}}{z_{st}}$. Two laws are often found. The first is a logarithmic law, $R_z \sim \log R_I$. The second law is a power law, $R_z \sim R_I^\beta$ with different exponent β for each system. b) Fold change detection (FCD) describes a system whose response depends only on the relative change in input signal and not the absolute level. Therefore, for a step increase from 1 to 2 and then from 2 to 4 the system response curve is exactly the same. doi:10.1371/journal.pcbi.1003781.g001

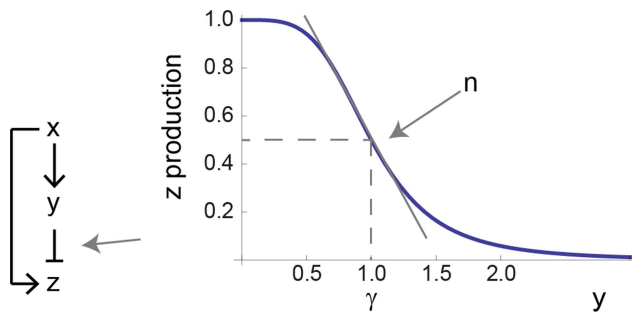


Figure 2. A model for the incoherent feed-forward loop includes three dimensionless parameters. In the incoherent type 1 feed-forward loop (I1-FFL) input X regulates an internal variable Y and both X and Y regulate Z . The repression of Z by Y is described by a Hill function with steepness n and half-way repression point γ . doi:10.1371/journal.pcbi.1003781.g002

separates to a product of one dimensional functions, $G(X, Y) = g(X)h(Y)$ [24], where $g(X)$ and $h(Y)$ are Hill functions (for more explanation see the Methods section). We therefore use a general form for the X dependence, $g(X)$, and multiply it by a repressive Hill function of Y (Eq. 2), with a maximal production rate β_z . The removal rate of Z is α_z . Here we consider step input functions in which X changes rapidly from one value to another. The values of $f(X)$ and $g(X)$ is determined by the step size in input.

For clarity, upper case letters relate to the elements in the circuit and lower case letters describe normalized model variables. The two-equation model (Eq. 1, 2) has 6 parameters. Dimensional analysis (fully described in Methods) reduces this to three dimensionless parameters (Eq. 3, 4).

The first parameter, γ , is the normalized half-way repression point of the output, defined by $\gamma \equiv \frac{K_{yz}}{Y_{st}^0}$, where Y_{st}^0 is the pre-step steady state level and K_{yz} is the level of Y needed to half-way repress Z . The second parameter is the cooperativity or steepness of the input function, n . The final parameter is the ratio of decay rates of Z and Y , $\rho \equiv \frac{\alpha_z}{\alpha_y}$. The normalized variables, $y \equiv \frac{Y}{Y_{st}^0}$ and $z \equiv \frac{Z}{\beta_z / \alpha_z g(X, t < 0)}$, are the new dimensionless variables in the model. Table 1 summarizes the parameters in the model for the I1-FFL.

This model for the I1-FFL describes the response to a step increase in input, starting from fully adapted conditions. We consider a change between an input level of $I_0 \equiv f(X, t < 0) = 1$, to a new level $I_1 \equiv f(X, t > 0) = F$. The step is thus characterized by the fold change F equal to the ratio between the initial and final input levels, $F = I_1 / I_0$.

In order for FCD to hold, the production rate of Z must be proportional to X^n ($g(X) \propto X^n$), where the power law exponent n is the same as the Hill coefficient that describes the steepness of the input function. In this way, the internal variable, Y , can precisely normalize out the fold change in input (see Methods). The model thus reads:

$$\dot{y} = F - y \quad (3)$$

$$\frac{1}{\rho} \dot{z} = F^n \frac{\gamma^n}{\gamma^n + y^n} - z \quad (4)$$

The higher γ , the more Y is needed to repress Z . The parameter n - the Hill coefficient of the input function - is important for this study, and determines the steepness of the regulation of the output Z by the internal variable Y (Fig. 2). The higher n the more steep the repression of Z by Y . The limit $n \rightarrow \infty$ resembles step-like regulation. Biochemical systems often have Hill coefficients in the range $n = 1 - 4$ [23]. The ratio between the removal rates, ρ , describes the relative time scale between Y and Z . For $\rho = 1$, Y and Z have the same removal rates, and for $\rho \gg 1$, the output Z is much faster than Y .

Goentoro et al. [15] showed, using a numerical parameter scan, that this circuit can perform FCD provided that threshold of the Z repression, K_{yz} , is small: that is $\gamma \rightarrow 0$. We therefore further analyze the limit of $\gamma \rightarrow 0$, meaning strong repression of Z , where the equation for the product Z (Eq. 4) becomes:

$$\frac{1}{\rho} \dot{z} \simeq F^n \frac{\gamma^n}{y^n} - z \quad (5)$$

In this limit, the system exhibits fold change detection since it obeys the sufficient conditions for FCD in Shoval et al (2010) (see Methods). We analytically solved the model (Eqs. 3, 5), in the limit of small γ , for all values of n , with initial conditions corresponding to steady state at the previous signal level, $y(0) = 1$, $z(0) = z_{st} = \gamma^n$ (in the limit $\gamma \rightarrow 0$). The solution (derived in Methods) is a decaying exponential multiplied by a term that contains a Beta function (Fig. 3a):

$$\frac{z(t)}{z_{st}} = e^{-\rho t} (1 + \rho \left(\frac{F-1}{F}\right)^\rho \text{B}\left(\frac{F-1}{F} e^{-t}, \frac{F-1}{F}, -\rho, 1-n\right)) \quad (6)$$

where the Beta function is $B(a, b, x, y) = \int_a^b u^{x-1} (1-u)^{y-1} du$. The dynamics of the output z shows a rise, reaches a peak z_{\max} , and then falls to the pre-signal steady state (Fig. 3a). At $t \rightarrow 0$ the solution is approximately linear with a slope that depends on F , n and ρ :

$$\frac{z(t)_{t \rightarrow 0}}{z_{st}} \simeq 1 + \rho(F^n - 1)t \quad (7)$$

At $t \rightarrow \infty$ the solution decays exponentially:

$$\frac{z(t)_{t \rightarrow \infty}}{z_{st}} \simeq 1 + e^{-\rho t} + n \frac{F-1}{F} e^{-t} \quad (8)$$

As in all FCD systems, exact adaptation is found. The error of exact adaptation, $\varepsilon \equiv \frac{z_{st}(F) - z_{st}(F=1)}{z_{st}(F=1)}$ goes as $\varepsilon \sim \gamma^n$ and vanishes at $\gamma \rightarrow 0$.

We explored how three main dynamical features depend on the input fold change F and the dimensionless parameters n and ρ . The first feature is the amplitude of the response, defined as the maximal point in the output z dynamics, z_{\max} . The second dynamical feature is the timing of the peak, t_{peak} . The third feature is the adaptation time, τ [25,26] which we define as the time it takes z to reach halfway between z_{\max} and its steady state (Fig. 3a). We denote R_I as the relative change in the input signal, $R_I = F - 1$ and $R_z = \frac{z_{\max} - z_{st}}{z_{st}}$ as the relative maximal amplitude of the response. Since ρ has only mild effects, we discuss it in the last section, and begin with $\rho = 1$, namely equal timescales for the two model variables.

Table 1. A parameter table for the I1-FFL model.

Parameter	Biological meaning	Definition
β_y	Maximal production rate of Y	
α_y	Removal rate of Y	
β_z	Maximal production rate of Z	
α_z	Removal rate of Z	
K_{yz}	Halfway repression point of Z by Y	
n	Steepness of input function	
Y_{st}^0	Pre-signal steady state of Y	$\frac{\beta_y}{\alpha_y} f(X, t < 0)$
γ	Normalized halfway repression point of Z by Y (dimensionless)	$\frac{K_{yz}}{Y_{st}^0}$
ρ	Removal rates ratio (dimensionless)	$\frac{\alpha_z}{\alpha_y}$

doi:10.1371/journal.pcbi.1003781.t001

A power law relation emerges when the cooperativity n of the input function is larger than one; Logarithmic behavior occurs when n equals one

We tested the effects of cooperativity in the input function, n , on the dynamics of the response. Cooperativity seems to have a weak effect on the timescales of the response: The adaptation time τ and the peak time t_{peak} decrease mildly with the fold F . For $\rho = 1$, the analytical solution of the time of the peak t_{peak} for all values of n is:

$$t_{peak} = \log \left(\frac{R_I}{1 + R_I} \left(1 + \frac{1}{(1 + R_z)^{1/n} - 1} \right) \right) \quad (\text{see derivation in Methods}).$$

Substituting the corresponding relative response, R_z , we receive a mildly decreasing function (Fig. 3b).

In contrast to the mild effect of cooperativity on timescales, cooperativity has a dramatic effect on the response amplitude. The maximal amplitude of the output z relative to its basal level, R_z , increases with the fold and behaves differently for each n . For low steepness, $n=1$, R_z increases in an approximately logarithmic manner with R_I (for $R_I \gg 1$), $R_z \sim \log(F-1) = \log R_I$ (normalized root-mean-square deviation, $\overline{RMSD} = 0.014$ for fitting to $a \log R_I + b$ compared to $\overline{RMSD} = 0.029$ for fitting to $a R_I^b$ - see Methods). More precisely the analytical solution is $R_z = \text{product log } \frac{R_z}{e}$ (see Methods) (Fig. 4a). The function $y = \text{product log}(x)$ is defined as the solution to the equation $x = ye^y$. The productlog function is approximately linear at $x \ll 1$, and approximately $\log(x)$ at $x \gg 1$.

For $n=2$, the peak response increases linearly $R_z \sim F-1 = R_I$. For $n=3$, the increase is approximately quadratic, $R_z \sim (F-1)^2 = R_I^2$ (Fig. 4b). We find that for any $n > 1$, the increase is approximately a power law with exponent $n-1$ in the limit of large R_I : $R_z \simeq \frac{1}{n-1} (F-1)^{n-1}$ (see Methods) ($\overline{RMSD} = 0.049, 0.003, 0.009$ for fitting to $\frac{1}{\beta} R_I^\beta$ compared to $\overline{RMSD} = 0.191, 0.436, 0.671$ for fitting to $a \log R_I + b$ for $n=2, 3, 4$ respectively). Note that the pre-factor in the power law is also predicted to depend simply on the Hill coefficient for $n > 1$, namely to be equal to $\frac{1}{n-1}$ (for $\rho = 1$). Indeed in fitting the numerical solution the best fit parameter is approximately $\beta \simeq n-1$: $\beta = 0.92, 1.99, 3.0$ for $n=2, 3, 4$ respectively. The dependence of output amplitude on input fold-change is thus a

power law, similar to Stevens power law, except for $n=1$ where the output dependence is logarithmic.

One point to consider regarding step input functions is that realistic inputs are not infinitely fast steps; however, a gradual change in input behaves almost exactly like an infinitely rapid step, as long as the timescale of the change in input is fast compared to the timescale of the Y and Z components. To demonstrate this, we computed the response to changes in input that have a timescale parameter α_x that can be tuned to go from very slow to very fast: $X(t) = 1 + (F-1) \tanh(\alpha_x t)$ (Fig. 5a). When $\alpha_x > \sim \alpha_y, \alpha_z$, the behavior of the relative maximal amplitude of the response, R_z , as a function of the relative change in the input signal, $R_I = F-1$, is very similar to the infinitely fast step solution (less than 5% difference for $F=50$, $n=\rho=1$ and $\frac{\alpha_x}{\alpha_y} = 10$, Fig. 5b). When the

change in input is much slower than the typical timescales of the circuit, the response is very small, since the signal is perceived almost as a steady-state constant. For slow changes in input, the I1-FFL response can be shown to be approximately proportional to the logarithmic temporal derivative of the signal [27–30].

A nonlinear integral feedback mechanism for FCD also shows a power law behavior

In addition to the I1-FFL mechanism, a non-linear integral feedback based mechanism (NLIFL) for FCD at small values of γ has been proposed by Shoval et al [11] (see Methods section) (Fig. 6a). This mechanism is found in models for bacterial chemotaxis [28]. The full model is described by:

$$\dot{Y} = kY(Z - Z_0) \quad (9)$$

$$\dot{Z} = \beta_z g(X) \frac{K_y^n}{K_y^n + Y^n} - \alpha_z Z \quad (10)$$

Its dimensionless equations following dimensional analysis (fully described in Methods) are:

$$\dot{y} = y \left(z - \frac{\gamma^n}{\gamma^n + 1} \right) \quad (11)$$

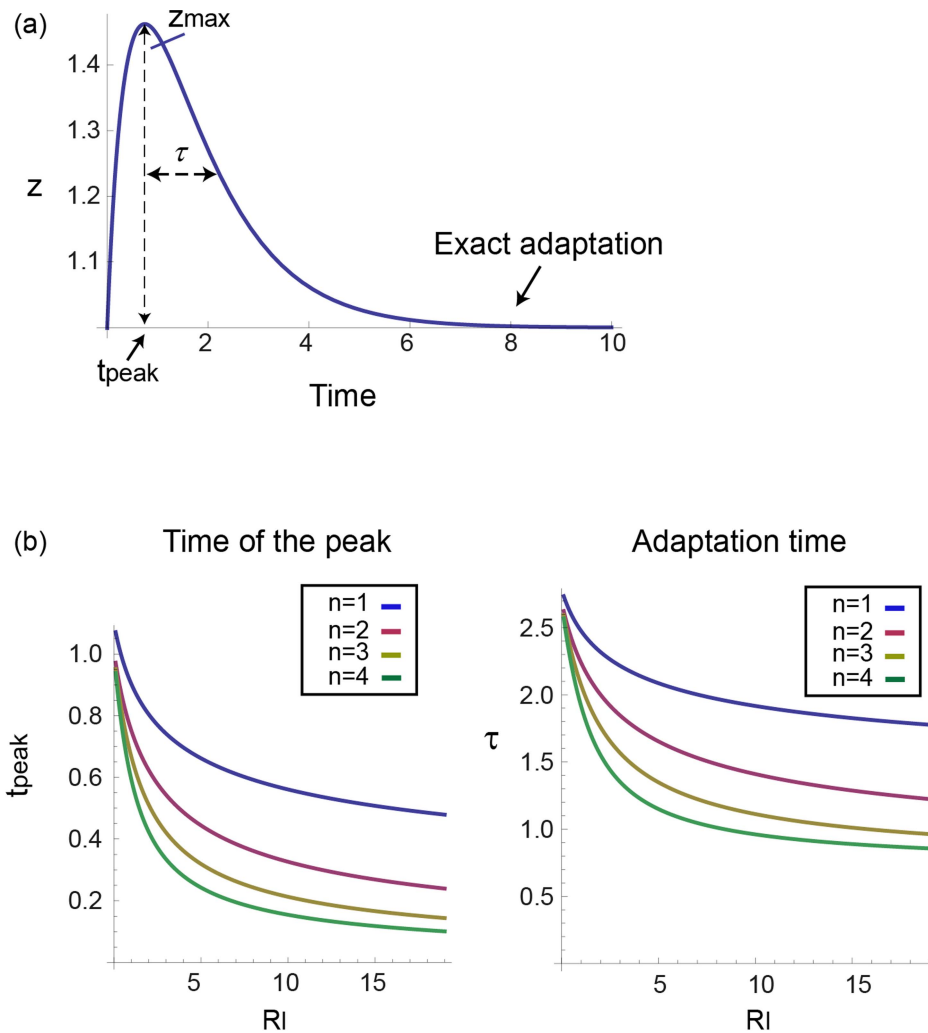


Figure 3. The I1-FFL shows FCD in the limit $\gamma \rightarrow 0$. a) Response to a step increase in input from I_0 to I_1 , which can be described by $R_I \equiv \frac{I_1 - I_0}{I_0} = F - 1$ where $F \equiv \frac{I_1}{I_0}$. The output dynamics show three features of interest: the amplitude of the peak response z_{\max} , the timing of the peak, t_{peak} and the adaptation time τ . b) The time scales of the response, the timing of the peak t_{peak} and the adaptation time τ , mildly decrease with the relative change in the input signal, R_I . The steepness, n , does not have a dramatic effect on this decrease. doi:10.1371/journal.pcbi.1003781.g003

$$\frac{1}{\rho} \dot{z} = F^n \frac{\gamma^n}{\gamma^n + y^n} - z \quad (12)$$

Where the new variables are: $y \equiv \frac{Y}{Y_{st}^0}$, $z \equiv \frac{Z}{Z_0} \frac{\gamma^n}{1 + \gamma^n}$ and the dimensionless parameters are defined as: $\gamma \equiv \frac{K_y}{Y_{st}^0}$ and $\rho \equiv \frac{\alpha_z^2}{k\beta_z g(X, t < 0)}$ (Methods). Table 2 summarizes the parameters in the model for the NLIFL.

We solved the NLIFL model (Eqs. 11, 12) numerically for the limit $\gamma \ll 1$ and find that the maximal response increases with the relative change in the signal in a power-law manner, $R_z \approx aR_I^\beta$ (Fig. 6b). The best-fit power law exponents increase with n , namely $\beta = 0.7, 1, 1.4, 1.8$ at $n = 1, 2, 3, 4$ for $\rho = 1$. A $\log R_I$ dependence does not fit the data at $n = 1$ ($RMSD = 0.01$ for fitting to aR_I^β compared to $RMSD = 0.18, 0.39, 0.55, 0.68$ for fitting to

$a \log R_I$ for $n = 1, 2, 3, 4$ respectively). To a good approximation, the power law is linearly related to the steepness parameter n , by $\beta = 0.1 + 0.46n$ (Fig. 6c).

The time scales in this circuit seem to decrease faster with the fold F for $n > 2$ than in the I1-FFL case, $t_{\text{peak}}, \tau \approx aR_I^\theta$ where $\theta_{t_{\text{peak}}} = -0.3, -0.6, -0.9, -1.3$ and $\theta_\tau = -0.3, -0.7, -1, -1.5$ at $n = 1, 2, 3, 4$ (Fig. 6d, all the fits of t_{peak}, τ have $R^2 > 0.99$).

Given the results so far, one can use the present approach to rule out certain mechanisms. If one observes a logarithmic dependence, one can draw at least two conclusions: (i) the NLIFL model addressed here can be rejected, (ii) if the I1-FFL model addressed here is at play, its steepness coefficient is $n = 1$.

If one observes a linear dependence of input on output, the I1-FFL and NLIFL mechanisms cannot be distinguished. The steepness can be inferred to be about $n = 2$ for both circuits.

Logarithmic law in eukaryotic signaling FCD

We applied the present approach to data from Takeda et al [17] on *Dictyostelium discoideum* chemotaxis. In these exper-

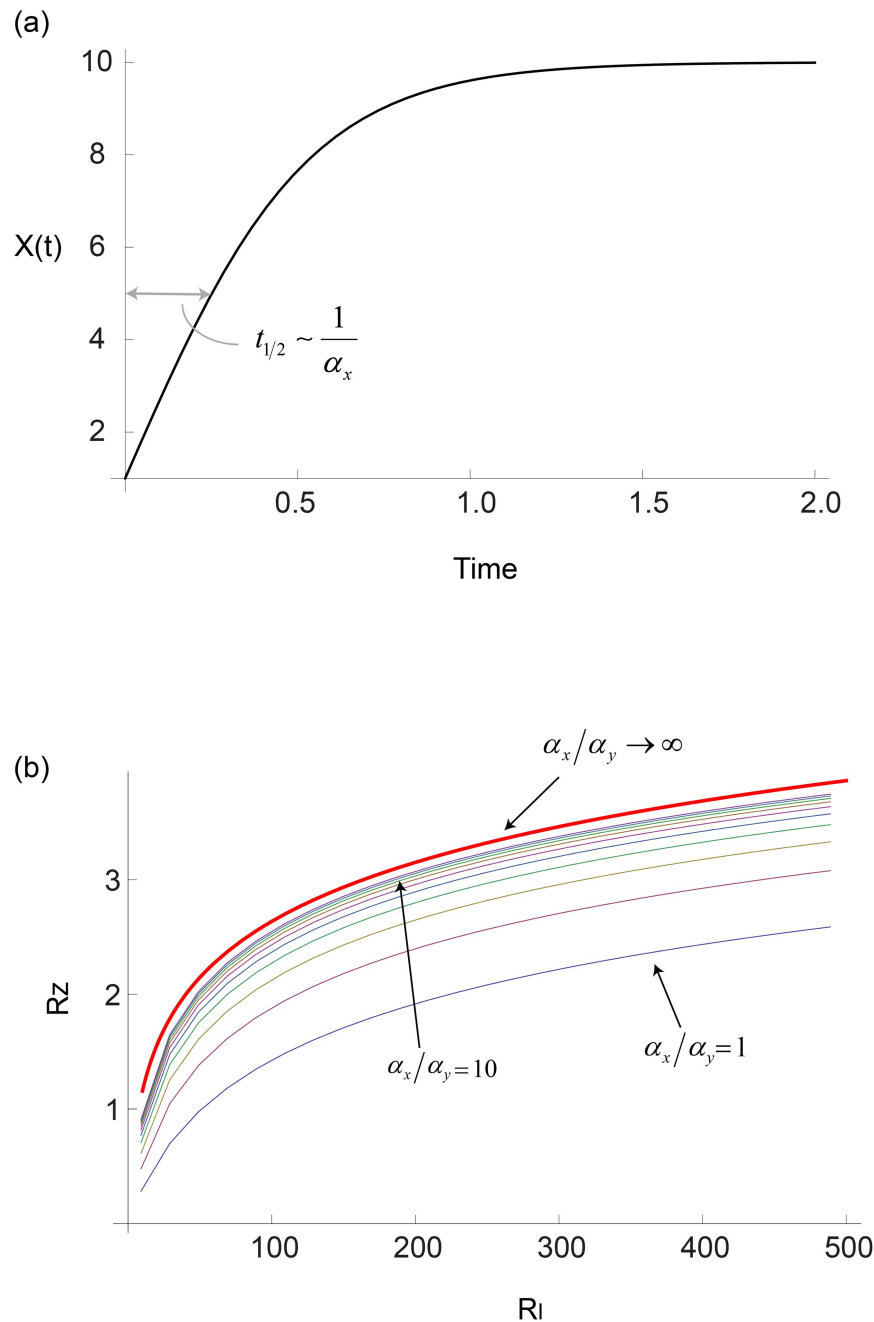


Figure 4. The response amplitude follows an approximately logarithmic law for $n=1$ and a power law at $n>1$. a) The numerical solution of the amplitude of the response, R_z , with $n=1$, is shown (blue dots) as well as its analytical solution $R_z = \text{product} \log \frac{R_I}{e}$ (blue curve) in a log-linear plot. A fit to $R_z = a \log R_I + b$ (red curve) captures the behavior better than a fit to $R_z = aR_I^b$ (green curve). b) For $n>1$ the numerical solution of the amplitude of the response, R_z , is shown (in dots) as function of R_I in a log-log plot. A fit to a power law behavior $R_z = \frac{1}{\beta} R_I^\beta$ with only one parameter (solid lines) describes the numerical results better than a fit to a logarithmic behavior $R_z = a \log R_I + b$ (dashed lines). At the limit of large R_I , $\beta \simeq n-1$. doi:10.1371/journal.pcbi.1003781.g004

iments, the input is cAMP steps applied to cells within a microfluidic system, and the output is a fluorescent reporter for Ras-GTP kinetics. The output showed nearly perfect adaptation and FCD-like response to a wide range of input cAMP steps. We re-drew the peak amplitude (Fig. 7a) and the time of peak (Fig. 7b) as a function of the added cAMP concentrations and find that it is well described by the analytical solution of the

maximal response and time of peak for an I1-FFL circuit with $n=1$. The peak amplitude (R_z) as a function of the relative input R_I is well described by a logarithmic relationship (mean-square weighted deviation, $MSWD=0.09$ for fitting the data to $a \log R_I + b$ considering the error-bars – see Methods). Fitting it to a power law aR_I^β results in a small exponent $\beta \simeq 0.12$ ($MSWD=0.11$) (Fig. 7c). Such a small power law

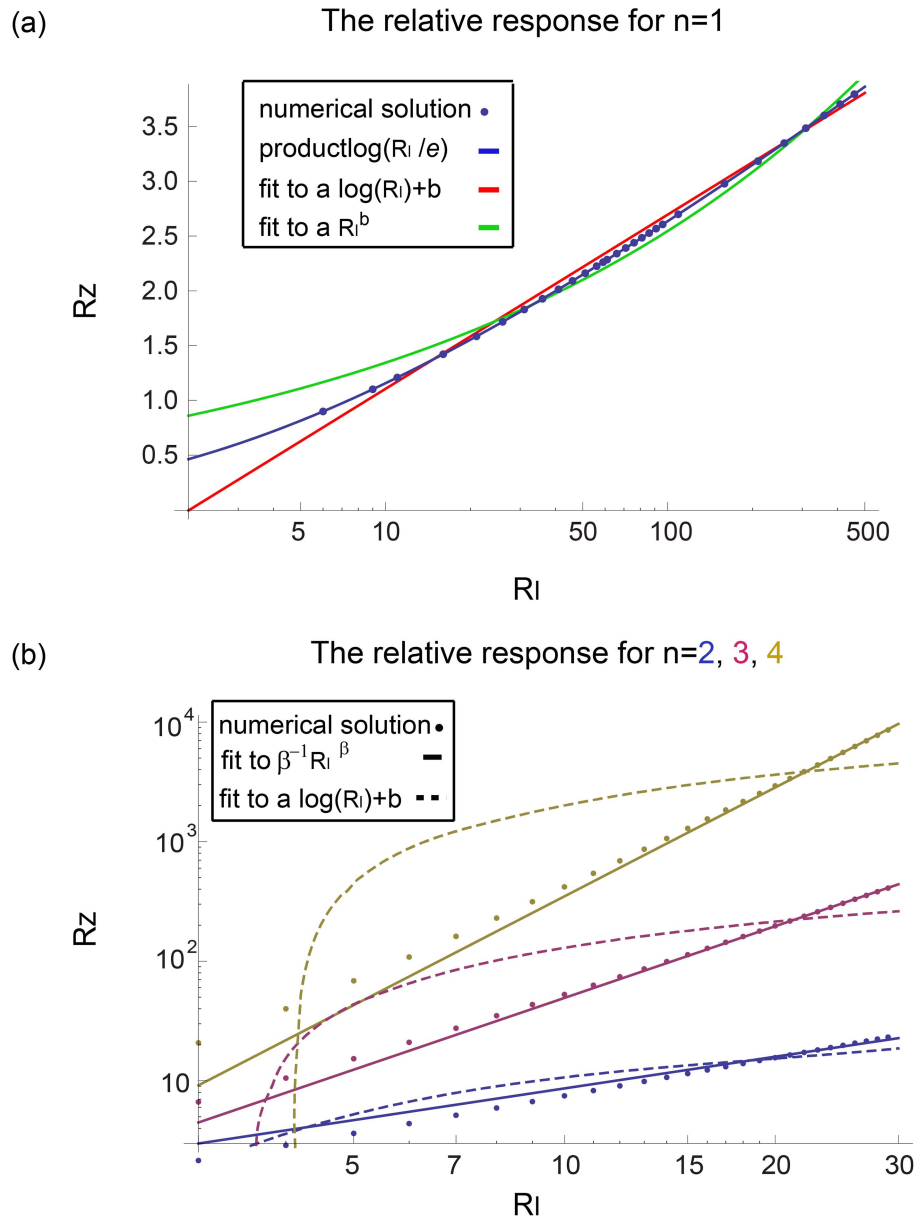


Figure 5. Rapidly changing input signal leads to responses similar to a step increase in signal; slowly changing input leads to weak response. a) Input signal with a tunable timescale, $X(t) = 1 + (F-1)\tanh(\alpha_x t)$ with $F=10$, $\alpha_x=2$. This signal goes from level 1 to level F , with a halfway time that goes as $1/\alpha_x$. b) The relative maximal amplitude, R_z , as a function of the relative change in the input signal R_I , is plotted for various values of the input timescale α_x . When the signal changes much faster than the timescale of the circuit, $\alpha_x \gg \alpha_y, \alpha_z$, the response is similar to the analytical solution for an infinitely fast step in input (Full red curve). When the timescale is slow, $\alpha_x \ll \alpha_y, \alpha_z$, the response of the circuit is weak. doi:10.1371/journal.pcbi.1003781.g005

exponent can only be obtained with a negative cooperativity in the NLIFL model considered here. Such negative cooperativity is rare in biological systems [31,32]. If we consider only positive cooperativity ($n \geq 1$), as found in most biological systems, the NLIFL model considered here provides a poor fit to the data ($\beta=0.7, MSWD=0.17$) (Fig. 7c).

Thus, the present analysis is most consistent with an I1-FFL mechanism considered here with $n=1$. The same is found when plotting the observed time-to-peak (t_{peak}) versus the analytical solution of the I1-FFL model ($t_{peak} = \log\left(\frac{R_I}{1+R_I} \left(1 + \frac{1}{(1+R_z)^{1/n} - 1}\right)\right)$)

with $n=1$ ($MSWD=0.02$ for fitting to a log $\left(\frac{R_I}{1+R_I} \left(1 + \frac{1}{\text{product log } \frac{R_I}{e}}\right)\right)$ (Fig. 7d). This agrees with the

numerical model fitting performed by Takeda et al, who conclude that an I1-FFL mechanism is likely to be at play (they used $n=1$ in their I1-FFL model, which is based on degradation of component Z by Y , rather than inhibition of production of Z by Y as in the present model).

In this analysis we assumed that the experimentally measured fluorescent reporter is in linear relation to the biological sensory

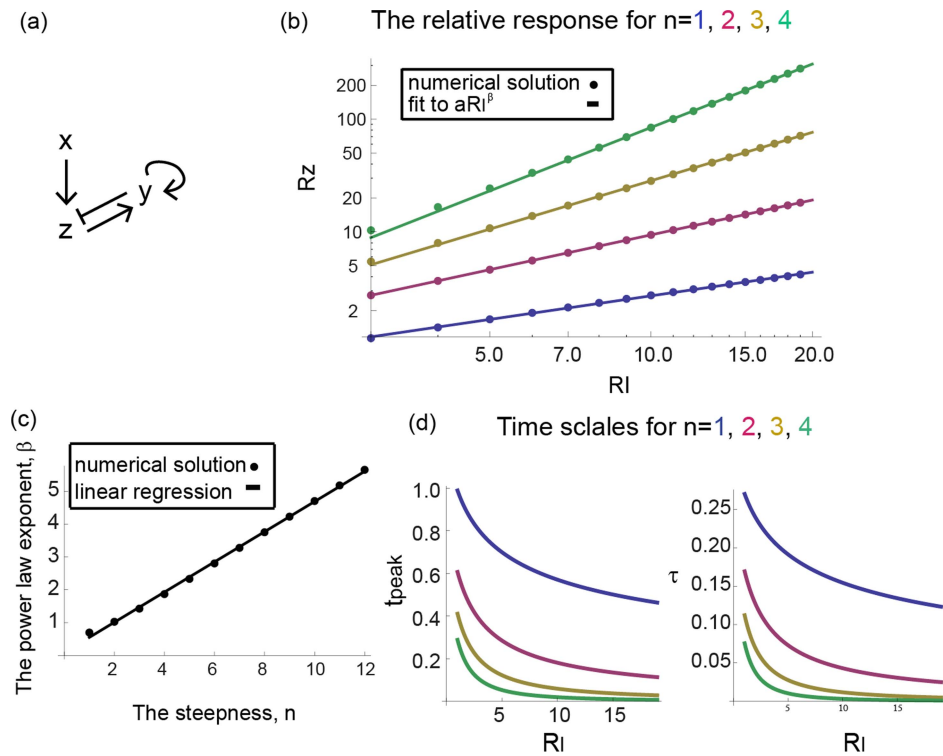


Figure 6. A different circuit showing FCD, the non-linear integral feedback loop (NLIFL), also exhibits a power law behavior. a) The NLIFL mechanism. b) The amplitude of the response is a power law of the relative change in input signal. c) The power-law exponent β increases linearly with n . d) The time-scales decrease faster with the fold change of the signal, R_I , and with n than in the incoherent feed-forward loop case (Fig. 3b).

doi:10.1371/journal.pcbi.1003781.g006

output, Ras activity. If this relation turns out to be nonlinear, the conclusions of this analysis must be accordingly modified.

Effect of timescale separation between the variables

In the eukaryotic chemotaxis system, the two model variables Y and Z have similar timescales ($\rho \equiv \alpha_z/\alpha_y \sim 1$). We also studied the effect of different timescales ($\rho \neq 1$), and find qualitatively similar results. A

logarithmic dependence of amplitude on F is found when $n=1$, and a power law when $n>1$. The power law β increases weakly with ρ (Fig. 8a). In the limit of very fast Z ($\rho \rightarrow \infty$), the solution approaches an instantaneous approximation (obtained by setting $\dot{z}=0$) in which the power law is n instead of $n-1$ (Fig. 8b). There is a cross over from the Stevens power law $\beta=n-1$ when $F \gg \rho$, to the instantaneous model power law $\beta=n$ when $1 \ll F \ll \rho$ (Fig. 8c). An analytical solution that exemplifies this crossover can be obtained at $n=1$, where

Table 2. A parameter table for the NLIFL model.

Parameter	Biological meaning	Definition
k		
Z_0	Steady state level of Z	
β_z	Maximal production rate of Z	
α_z	Removal rate of Z	
K_y	Halfway repression point of Z by Y	
n	Steepness of input function	
Y_{st}^0	Pre-signal steady state of Y	$K_y \left(\frac{\beta_z g(X, t < 0)}{\alpha_z Z_0} - 1 \right)^{1/n}$
γ	Normalized halfway repression point of Z by Y (dimensionless)	$\frac{K_y}{Y_{st}^0}$
ρ	Timescale ratio (dimensionless)	$\frac{\alpha_z^2}{k\beta_z g(X, t < 0)}$

doi:10.1371/journal.pcbi.1003781.t002

$R_z = \rho \text{productlog}\left(\frac{R_I}{\rho e}\right)$ (Methods). Because of the limit behavior of the *productlog* function mentioned above, at small fold values $R_z \sim R_I$, and at large values $R_z \sim \log R_I$. In summary, the instantaneous approximation, commonly used in biological modeling, must be done with care in the case of FCD systems.

Discussion

This study explored how two common biophysical laws, logarithmic and power-law, can stem from mechanistic models of sensing. We consider two of the best studied fold-change detection mechanisms, and find that a single model parameter controls which law is found: the steepness n of the effect of the internal variable on the output. We solved the dynamics analytically for the I1-FFL mechanism, finding that logarithmic-like input-output relations occurs when $n=1$, and power-law occurs when $n>1$, with power law $\beta \cong n-1$, and prefactor $\frac{1}{n-1}$ at $\rho=1$. The nonlinear integral feedback loop (NLIFL) mechanism - a second class of mechanisms to achieve FCD - can only produce a power law. Thus, if one observes logarithmic behavior, one can rule out the specific NLIFL mechanism considered here. This appears to be the case in experimental data on eukaryotic chemotaxis [17], in which good

agreement is found to the present results in the I1-FFL mechanism with $n=1$ in both peak response and timing.

This theory gives a prediction about the internal mechanism for sensory systems based on the observed laws that connect input and output signals. Thus, by measuring the system response to different folds in the input signal one may infer the cooperativity of the input function and potentially rule out certain classes of mechanism. For example, if a linear dependence of amplitude on fold change is observed (power law with exponent $\beta=1$), one can infer that the steepness coefficient is about $n=2$ for both the specific I1-FFL and NLIFL circuits considered here, with slight modification if the timescales of variables are unequal. Such a linear detection of fold changes may occur in drosophila development of the wing imaginal disk [33–35].

The problem of finding the FCD response amplitude shows a feature of technical interest for modeling biological circuits. In many modeling studies, a quasi-steady-state approximation, also called an instantaneous approximation, is used when a separation of timescales exists between processes. In this approximation, one replaces the differential equation for the fast variables by an algebraic equation, by setting the temporal derivative of the fast variable to zero. This approximation results in simpler formulae, and is often very accurate, for example in estimating Michaelis-Menten enzyme steady states [36]. However, as noted by Segel et al [36], this approximation is invalid to

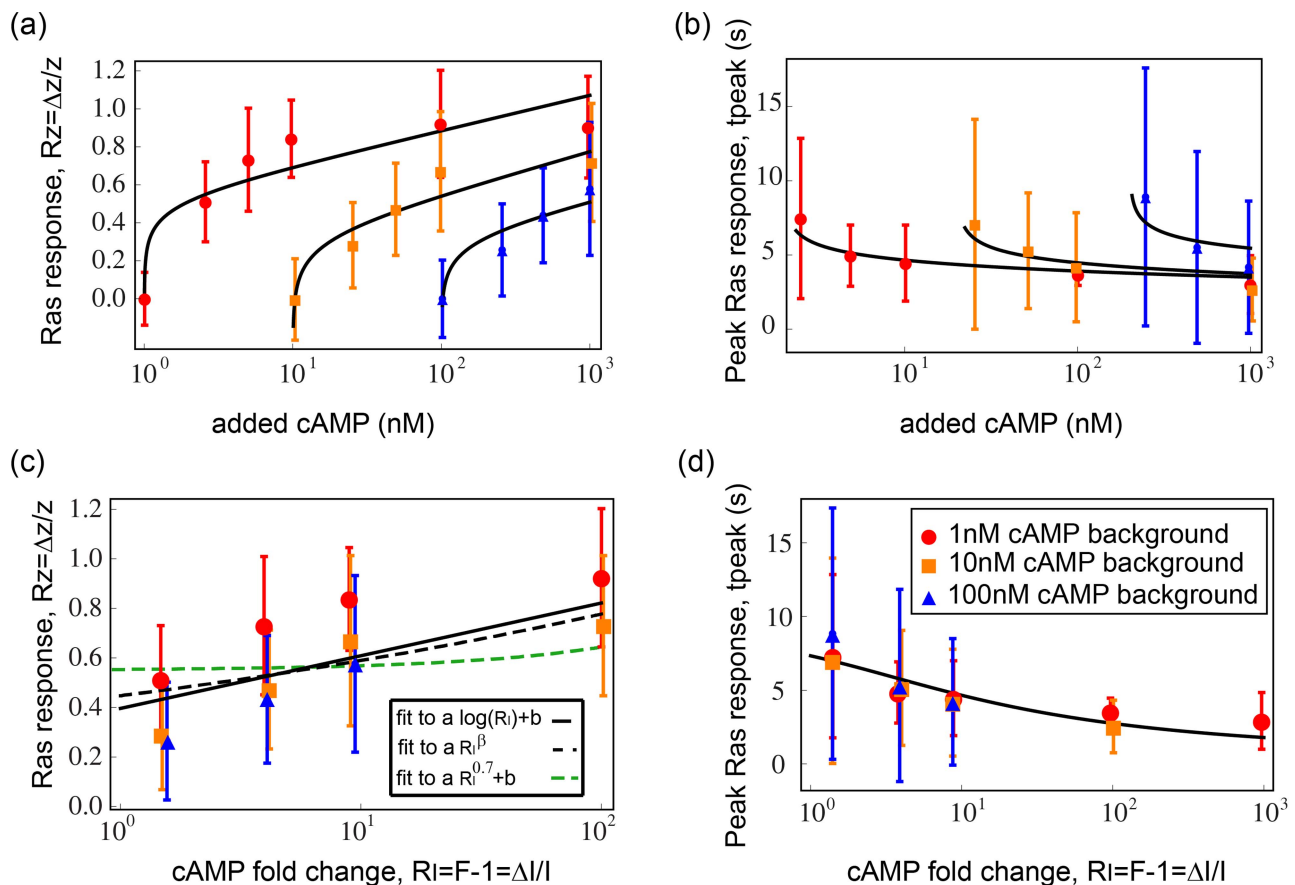


Figure 7. A mechanism of eukaryotic signaling FCD illustrates this theory. a) The response of Ras-GTP to different concentrations of added cAMP in *Dictyostelium discoideum* chemotaxis is re-plotted together with the timing of the peak (b). A logarithmic function describes the data well. The black lines are our fit to the data. c) The response of Ras-GTP is re-plotted as function of the different fold changes in cAMP concentrations. The solid line is a fit to $R_z = a \log R_I + b$, the black dashed line is a fit to $R_z = a R_I^\beta$ and the green dashed line is a fit to a power law with exponent $\beta=0.7$. d) The corresponding solution for the timing of the peak for I1-FFL with $n=1$ explains well the data. doi:10.1371/journal.pcbi.1003781.g007

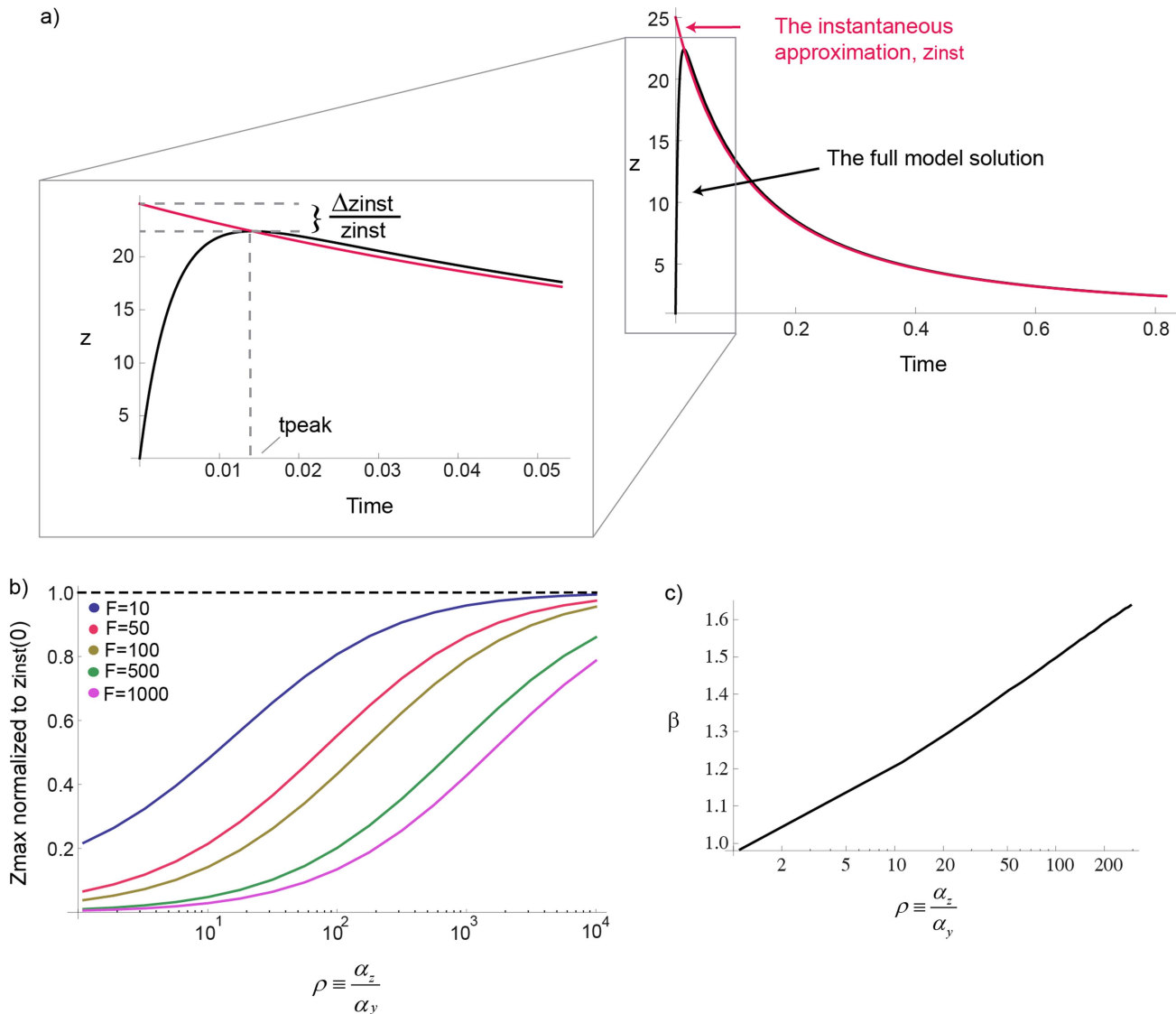


Figure 8. The instantaneous approximation does not capture the correct amplitude behavior. a) The power law for $n=1$ increases mildly with ρ to a value between 1 and 2. b) The instantaneous approximation (in red) and the full model solution (in black) are plotted as function of time for $F=5$, $n=2$, $\rho \approx 250$. c) The maximal response z_{max} normalized to $z_{\text{inst}}^{\text{max}} = F^n$ is plotted for different folds and for $n=1$. The error between the maxima of the instantaneous approximation and the full model increases with the fold F . doi:10.1371/journal.pcbi.1003781.g008

describe transients on the fast time scale. In the present study, we are interested in the maximal amplitude of the FCD circuits. In some input regimes, namely $F \gg \rho$, the instantaneous approximation predicts an incorrect power law. To obtain accurate estimates, the full set of equations must be solved without setting derivatives to zero.

It would be interesting to use the present approach to analyze experiments on other FCD systems, and to gain mechanistic understanding of sensory computations.

Methods

The two dimensional input function can be considered as a product of one dimensional input functions

Consider a general partition function for an input function with an activator and a repressor: $G(X, Y) = \frac{aX^n}{1 + \beta X^n + \gamma Y^m + \delta X^n Y^m}$.

The regime in which FCD applies is that of strong repression, $\gamma Y^m \gg 1$ and non-saturated activation $\beta X^n \ll 1$ [10]. In this limit, $G(X, Y) \approx \frac{aX^n}{\gamma Y^m}$, and is thus well approximated by a product.

More generally, $G(X, Y)$ is a product of two functions whenever binding is independent, $G(X, Y) = \frac{aX^n}{1 + \beta X^n} \frac{1}{1 + \gamma Y^m} = \frac{aX^n}{1 + \beta X^n + \gamma Y^m + \beta \gamma X^n Y^m}$, which occurs when the relation $\delta = \beta \gamma$ holds. The biological meaning of the relation is that X and Y bind the Z promoter independently so that the probability of X to bind the promoter and the probability of Y to unbind equals the multiplication of the probabilities:

$$P(\text{Xbound} \wedge \text{Yunbound}) = P(\text{Xbound})P(\text{Yunbound}).$$

In the NLIFL case, one can show from the MWC model chemotaxis by Yu Berg et al [28] that in the FCD regime it is simply a power law.

Dimensional analysis of the full model for I1-FFL and NLIFL

We performed dimensional analysis of the full model of the I1-FFL (Eq. 1, 2) by rescaling as many variables as possible. The rescaled variables:

$$y \equiv \frac{Y}{Y_{st}^0} \quad (\text{M1})$$

$$z \equiv \frac{Z}{\beta_z/\alpha_z g(X, t < 0)}$$

Where Y_{st}^0 is the pre-signal steady state of Y, derived by taking $\dot{Y}=0$: $Y_{st}^0 = \frac{\beta_y}{\alpha_y} f(X, t < 0)$, and $Z_{st} = \frac{\beta_z}{\alpha_z} g(X) \frac{K_{yz}^n}{K_{yz}^n + Y_{st}^n}$ is the steady state of Z derived by taking $\dot{Z}=0$. Substituting these rescaled variables we receive:

$$\frac{\dot{Y}}{Y_{st}^0} = \alpha_y \frac{f(X)}{f(X, t < 0)} - \alpha_y \frac{Y}{Y_{st}^0} \quad (\text{M2})$$

$$\frac{\dot{Z}}{\beta_z/\alpha_z g(X, t < 0)} = \alpha_z \frac{g(X)}{g(X, t < 0)} \frac{K_{yz}^n}{K_{yz}^n + Y^n} - \alpha_z \frac{Z}{\beta_z/\alpha_z g(X, t < 0)}$$

Since we assume that $f(X)$ is determined by the step size in input, we can consider merely the fold change F in input, $F \equiv \frac{f(X)}{f(X, t < 0)}$.

For FCD to hold we consider $F^n \equiv \frac{g(X)}{g(X, t < 0)}$. Defining the rescaled repression threshold $\gamma \equiv \frac{K_{yz}^n}{Y_{st}^0}$ we receive in the new rescaled variables (lower case letters y and z):

$$\frac{1}{\alpha_y} \dot{y} = F - y \quad (\text{M3})$$

$$\frac{1}{\alpha_z} \dot{z} = F^n \frac{\gamma^n}{\gamma^n + y^n} - z$$

Rescaling the time to $t \rightarrow \alpha_y t$ and defining $\rho \equiv \frac{\alpha_z}{\alpha_y}$ yields to Eq. 3, 4 in the main text.

We also performed dimensional analysis of the full model of the NLIFL (Eqs. 9, 10) by rescaling as many variables as possible. The rescaled variables:

$$y \equiv \frac{Y}{Y_{st}^0} \quad (\text{M4})$$

$$z \equiv \frac{Z}{Z_0} \frac{\gamma^n}{1 + \gamma^n}$$

Where Y_{st}^0 is the pre-signal steady state of Y, derived by taking $\dot{Z}=0$ and assuming $Z_{st} = Z_0$: $Y_{st}^0 = K_y \left(\frac{\beta_z g(X, t < 0)}{\alpha_z Z_0} - 1 \right)^{1/n}$, and $\gamma \equiv \frac{K_y}{Y_{st}^0} = \left(\frac{\beta_z g(X, t < 0)}{\alpha_z Z_0} - 1 \right)^{-1/n}$. Substituting these rescaled variables we receive:

$$\frac{1}{kZ_0} \frac{\gamma^n}{1 + \gamma^n} \dot{Y} = \frac{Y}{Y_{st}^0} \left(\frac{Z}{Z_0} \frac{\gamma^n}{1 + \gamma^n} - \frac{\gamma^n}{1 + \gamma^n} \right) \quad (\text{M5})$$

$$\frac{\dot{Z}}{Z_0} \frac{\gamma^n}{1 + \gamma^n} = \frac{\beta_z}{Z_0} \frac{\gamma^n}{1 + \gamma^n} g(X) \frac{K_{yz}^n}{K_{yz}^n + Y^n} - \alpha_z \frac{\gamma^n}{1 + \gamma^n} \frac{Z}{Z_0}$$

After algebraic manipulation and in the new rescaled variables (lower case letters y and z):

$$\frac{1}{kZ_0} \frac{\gamma^n}{1 + \gamma^n} \dot{y} = y \left(z - \frac{\gamma^n}{1 + \gamma^n} \right) \quad (\text{M6})$$

$$\frac{1}{\alpha_z} \dot{z} = \frac{g(X)}{g(X, t < 0)} \frac{\gamma^n}{\gamma^n + y^n} - z$$

We consider here also $F^n \equiv \frac{g(X)}{g(X, t < 0)}$.

Rescaling the time to $t \rightarrow kZ_0 \frac{1 + \gamma^n}{\gamma^n} t = \frac{g(X, t < 0) \beta_z}{\alpha_z} kt$ and defining $\rho \equiv \frac{\alpha_z^2}{k\beta_z g(X, t < 0)}$ yields to Eqs. 11, 12 in the main text.

Proof that FCD holds in the model for I1-FFL and NLIFL

Given a set of ordinary differential equations with internal variable y, input F and output z:

$$\dot{y} = f(y, z, F) \quad (\text{M7})$$

$$\dot{z} = g(y, z, F) \quad (\text{M8})$$

According to Shoal et. al. (2010), FCD holds if the system is stable, shows exact adaptation and g and f satisfy the following homogeneity conditions for any $p > 0$:

$$f(py, z, pF) = pf(y, z, F) \quad (\text{M9})$$

$$g(py, z, pF) = g(y, z, F) \quad (\text{M10})$$

In the model for I1-FFL (Eq. 3, 4) at the limit of strong repression $\gamma \rightarrow 0$:

$$f(py, z, pF) = (pF - py) = pf(y, z, F)$$

$$\frac{1}{\rho} g(py, z, pF)_{\gamma \rightarrow 0} \cong (pF)^n \frac{\gamma^n}{(py)^n} - z = F^n \frac{\gamma^n}{y^n} - z = g(y, z, F)_{\gamma \rightarrow 0}$$

Exact adaptation also holds at $\gamma \rightarrow 0$, $z_{st} \simeq z_0$. This holds also for the NLIFL (Eqs. 9, 10).

Analytical solution for the I1-FFL

The solution for y is an exponent:

$$y(t) = e^{-t} + F(1 - e^{-t}) \quad (\text{M11})$$

The general solution for the ODE $\dot{z} = f(t) - z$ with the initial condition $z(0) = z_0$ is:

$$z(t) = z_0 e^{-t} + e^{-t} \int_0^t e^{\tau} f(\tau) d\tau \quad (\text{M12})$$

For our model Eq. M12 reads:

$$z(t) = \gamma^n e^{-\rho t} + \gamma^n \rho e^{-\rho t} \int_0^t e^{\tau} F^n \frac{1}{(e^{-\tau} + F(1 - e^{-\tau}))^n} d\tau \quad (\text{M13})$$

By changing the variable in the integral in Eq. M13: $w = e^{\tau} \frac{F}{F-1}$ we get:

$$z(t) = \gamma^n e^{-\rho t} \left(1 + \rho \left(\frac{F-1}{F}\right)^{\rho} \int_{\frac{F-1}{F} e^{-t}}^{\frac{F-1}{F}} w^{-\rho-1} (1-w)^{-n} dw\right) \quad (\text{M14})$$

Which is by definition the solution in Eq. 6.

Analytical solution for the time of peak for the I1-FFL

At the time of peak $\dot{z} = 0$, therefore from Eq. 5 in the main text we get:

$$z(t_{peak}) = \left(\frac{F\gamma}{y(t_{peak})}\right)^n \quad (\text{M15})$$

From our definition of the relative response $R_z \equiv \frac{z(t_{peak}) - z_{st}}{z_{st}}$ we have:

$$y(t_{peak}) = \frac{F}{(R_z + 1)^{1/n}} \quad (\text{M16})$$

Substituting the solution of y (Eq. M11) and by algebraic manipulation we receive the analytical solution for t_{peak} :

$$t_{max} = \log \left(\frac{R_I}{1 + R_I} \left(1 + \frac{1}{(1 + R_z)^{1/n} - 1} \right) \right) \quad (\text{M17})$$

Analytical solution for the maximal response

The analytical results were derived by taking the derivative of the solution for $z(t)$ (Eq. 6 in the main text) and substituting time of the peak (Eq. M17), $\frac{dz(t_{peak})}{dt} = 0$. This provides an equation for

the amplitude of the maximal response, $f(R_z, R_I, n, \rho) = 0$, yielding an intractable equation:

$$f(R_z, R_I, n, \rho) = \left(\frac{1+R_I}{R_I}\right)^{\rho} - (1+R_z) \left(1 - \frac{1}{(1+R_z)^{1/n}}\right)^{-\rho} \dots + \rho(-1)^n B\left(\frac{1+R_I}{R_I}, \left(1 - \frac{1}{(1+R_z)^{1/n}}\right)^{-1}, \rho+n, 1-n\right) = 0 \quad (\text{M18})$$

Where we used the identity: $B(a, b, -\rho, 1-n) = (-1)^n B(b^{-1}, a^{-1}, \rho+n, 1-n)$. This identity can be easily proven by using the change of variable, $w \equiv \frac{1}{u}$, in the integral of the Beta function.

For $n=1$ Eq. M18 becomes:

$$\left(\frac{1+R_I}{R_I}\right)^{\rho} - (1+R_z) \left(\frac{1+R_z}{R_z}\right)^{\rho} - \rho B\left(\frac{1+R_I}{R_I}, \frac{1+R_z}{R_z}, \rho+1, 0\right) = 0 \quad (\text{M19})$$

Using the Series function of Mathematica to expand Eq. M19 in the limit of large R_I , R_z and keeping high orders in R_I , R_z yields:

$$1 - \left(1 + \frac{1}{R_z}\right)^{\rho} (1+R_z) - \rho \log\left(\frac{R_z}{R_I}\right) = 0 \quad (\text{M20})$$

Using $\left(1 + \frac{1}{x}\right)^a \simeq 1 + \frac{a}{x}$ in the limit of large x we receive:

$$-R_z - \rho - \rho \log\left(\frac{R_z}{R_I}\right) = 0 \quad (\text{M21})$$

Taking the exponent of this Eq. M21 yields:

$$\frac{R_I}{\rho e} = \frac{R_z}{\rho} e^{R_z/\rho} \quad (\text{M22})$$

The solution for Eq. M22 is by definition the productlog function: $R_z = \rho \text{product log}\left(\frac{R_I}{\rho e}\right)$.

For $\rho=1$ Eq. M18 becomes:

$$\left(\frac{1+R_I}{R_I}\right) - (1+R_z) \left(\frac{1+R_z}{R_z}\right) - B\left(\frac{1+R_I}{R_I}, \frac{1+R_z}{R_z}, 2, 0\right) = 0 \quad (\text{M23})$$

Since $B(a, b, 2, 0) = \int_a^b \frac{x}{1-x} dx = -(b-a) - \log\left(\frac{1-b}{1-a}\right)$, Eq. M23 yields:

$$\left(\frac{1+R_I}{R_I}\right) - (1+R_z) \left(\frac{1+R_z}{R_z}\right) - \left(\frac{1}{R_I} - \frac{1}{R_z} + \log\left(\frac{R_z}{R_I}\right)\right) = 0 \quad (\text{M24})$$

By algebraic manipulation Eq. M24 becomes $1 + R_z + \log\left(\frac{R_z}{R_I}\right) = 0$. Taking the exponent of this equation yields:

$$\frac{R_I}{e} = R_z e^{R_z} \quad (\text{M25})$$

The solution for Eq. M25 is by definition the productlog function:

$$R_z = \text{product log} \left(\frac{R_I}{e} \right).$$

For $n > 1, \rho = 1$ we define $\xi \equiv (1 + R_z)^{1/n} - 1$, substituting this new variable into Eq. M18 we have:

$$\frac{1 + R_I}{R_I} - (1 + \xi)^n \frac{1 + \xi}{\xi} + (-1)^n B \left(\frac{1 + R_I}{R_I}, \frac{1 + \xi}{\xi}, 1 + n, 1 - n \right) = 0 \quad (\text{M26})$$

Using the Series function of Mathematica for large R_I and ξ yields:

$$-(1 + n)R_I^n \xi^2 - R_I^{n+1} \xi^2 + R_I^2 \xi^n (1 + n + \xi) + (n - 1)R_I^2 \xi (-\xi + (1 + \xi)^{n+1}) = 0 \quad (\text{M27})$$

Keeping the highest order in R_I and ξ we receive: $(n - 1)\xi^n \approx R_I^{n-1}$. Recall that $\xi^n \approx (1 + \xi)^n \equiv 1 + R_z \approx R_z$ for large R_z and ξ , and therefore $R_z \approx \frac{1}{n-1} R_I^{n-1}$.

The instantaneous approximation does not capture the correct amplitude behavior

For the instantaneous approximation to be true at large ρ , the error, $\frac{\Delta z_{inst}}{z_{inst}}$ (Fig. 8a), between the maximal amplitude in the instantaneous approximation and the full model should vanish at $\rho \rightarrow \infty$.

$$\frac{\Delta z_{inst}}{z_{inst}} \approx \frac{1}{z_{inst}(0)} \left(\frac{dz_{inst}}{dt} \right)_{t=0} t_{peak} \sim (F - 1) t_{peak}(F) \quad (\text{M28})$$

Where $t_{peak}(F)$ decrease with F slower than F^{-1} , therefore $\frac{\Delta z_{inst}}{z_{inst}} \sim f(F)$ with $f(F)$ a monotonic increasing function of F . This proves that even at large ρ , the error increases with F (Fig. 8b) and can be very large.

References

- Ernst Heinrich Weber (1905) *Tatsinn und Gemeingefühl*. Verl Von Wilhelm Englemann Leipzig Ger.
- Stanley Smith Stevens (1957) On the psychophysical law. *Psychol Rev* 64: 153–181.
- Thoss F (1986) Visual threshold estimation and its relation to the question: Fechner-law or Stevens-power function. *ACTA NEUROBIOL EXP* 46: 303–310.
- Krueger LE (1989) Reconciling Fechner and Stevens: Toward a unified psychophysical law. *Behav Brain Sci* 12: 251–320.
- Nizami L (2009) A Computational Test of the Information-Theory Based-Entropy Theory of Perception: Does It Actually Generate the Stevens and Weber-Fechner Laws of Sensation? *Proceedings of the World Congress on Engineering*. Vol. 2. Available: http://iaeng.org/publication/WCE2009/WCE2009_pp1853-1858.pdf. Accessed 16 October 2013.
- Chater N, Brown GD (1999) Scale-invariance as a unifying psychological principle. *Cognition* 69: B17–B24.
- Copelli M, Roque AC, Oliveira RF, Kinouchi O (2002) Physics of psychophysics: Stevens and Weber-Fechner laws are transfer functions of excitable media. *Phys Rev E* 65: 060901. doi:10.1103/PhysRevE.65.060901.
- Billock VA, Tsou BH (2011) To honor Fechner and obey Stevens: Relationships between psychophysical and neural nonlinearities. *Psychol Bull* 137: 1.
- Tzur G, Berger A, Luria R, Posner MI (2010) Theta synchrony supports Weber-Fechner and Stevens' Laws for error processing, uniting high and low mental processes. *Psychophysiology* 47: 758–766. doi:10.1111/j.1469-8986.2010.00967.x.
- Goentoro L, Shoval O, Kirschner MW, Alon U (2009) The incoherent feedforward loop can provide fold-change detection in gene regulation. *Mol Cell* 36: 894–899.
- Shoval O, Goentoro L, Hart Y, Mayo A, Sontag E, et al. (2010) Fold-change detection and scalar symmetry of sensory input fields. *Proc Natl Acad Sci* 107: 15995–16000.

Fits and numerical simulations

All the numeric simulations and fits were made in Mathematica 9.0.

The root-mean-square deviation (RMSD) [37] calculated for comparing the goodness of fit between the two models is defined

$$\text{as: } RMSD = \frac{1}{\bar{x}_{numeric}} \sqrt{\frac{1}{n} \sum_{i=1}^n r_i^2}, r_i \equiv x_{i,numeric} - x_{i,model}.$$

The data points from Takeda et al were extracted by using the 'ginput' function of MATLAB. The fits for the data were made using the NonlinearModelFit function considering the error-bars,

$$\Delta x_i, \text{ as weights, } w_i = \frac{1}{\Delta x_i^2}.$$

The goodness of fit was tested using the mean-square weighted deviation (MSWD) [37] which sums the residuals (r) - sum of squares of errors with weights of $1/s.d.$: $MSWD =$

$$\frac{1}{n-1} \sum_{i=1}^n w_{ii} r_i^2, w_{ii} = \frac{1}{\Delta x_i^2}.$$

Note on biophysical law terminology

We define logarithmic response as $\frac{\Delta z}{z} = \log \frac{\Delta I}{I}$. In contrast, traditional definition of the Weber-Fechner law (also called the Fechner law) in biophysics is (e.g. ref. [3]) as $\Delta z \sim \log I$. Thus the present definition concerns relative change in input and output, whereas the Weber-Fechner law concerns absolute input and output. Note also that the Weber-Fechner law is distinct from Weber's law, on the just noticeable difference in sensory systems, whose relation to FCD was discussed in Ref [11].

Acknowledgments

We thank all members of our lab for discussions.

Author Contributions

Analyzed the data: MA AM UA. Contributed reagents/materials/analysis tools: MA AM UA. Wrote the paper: MA AM UA.

- Lazova MD, Ahmed T, Bellomo D, Stocker R, Shimizu TS (2011) Response rescaling in bacterial chemotaxis. *Proc Natl Acad Sci* 108: 13870–13875.
- Masson J-B, Voisinne G, Wong-Ng J, Celani A, Vergassola M (2012) Noninvasive inference of the molecular chemotactic response using bacterial trajectories. *Proc Natl Acad Sci* 109: 1802–1807.
- Cohen-Saidon C, Cohen AA, Sigal A, Liron Y, Alon U (2009) Dynamics and variability of ERK2 response to EGF in individual living cells. *Mol Cell* 36: 885–893.
- Goentoro L, Kirschner MW (2009) Evidence that fold-change, and not absolute level, of β -catenin dictates Wnt signaling. *Mol Cell* 36: 872–884.
- Skataric M, Sontag E (2012) Exploring the scale invariance property in enzymatic networks. *Decision and Control (CDC), 2012 IEEE 51st Annual Conference on*. pp. 5511–5516. Available: http://ieeexplore.ieee.org/xpls/abs_all.jsp?arnumber=6426990. Accessed 16 October 2013.
- Takeda K, Shao D, Adler M, Charest PG, Loomis WF, et al. (2012) Incoherent feedforward control governs adaptation of activated Ras in a eukaryotic chemotaxis pathway. *Sci Signal* 5: ra2.
- Hart Y, Mayo AE, Shoval O, Alon U (2013) Comparing Apples and Oranges: Fold-Change Detection of Multiple Simultaneous Inputs. *PLoS One* 8: e57455.
- Mangan S, Alon U (2003) Structure and function of the feed-forward loop network motif. *Proc Natl Acad Sci* 100: 11980–11985.
- Wang P, Lü J, Ogorzalek MJ (2012) Global relative parameter sensitivities of the feed-forward loops in genetic networks. *Neurocomputing* 78: 155–165.
- Widder S, Solé R, Macía J (2012) Evolvability of feed-forward loop architecture biases its abundance in transcription networks. *BMC Syst Biol* 6: 7.
- Levchenko A, Iglesias PA (2002) Models of Eukaryotic Gradient Sensing: Application to Chemotaxis of Amoebae and Neutrophils. *Biophys J* 82: 50–63. doi:10.1016/S0006-3495(02)75373-3.
- Alon U (2007) *An Introduction to Systems Biology: Design Principles of Biological Circuits* (Mathematical and Computational Biology Series vol 10).

- Boca Raton, FL: Chapman and Hall. Available: <http://www.lavoisier.fr/livre/notice.asp?ouvrage=1842587>. Accessed 9 April 2013.
24. Kaplan S, Bren A, Zaslaver A, Dekel E, Alon U (2008) Diverse two-dimensional input functions control bacterial sugar genes. *Mol Cell* 29: 786–792. doi:10.1016/j.molcel.2008.01.021.
 25. Alon U, Surette MG, Barkai N, Leibler S (1999) Robustness in bacterial chemotaxis. *Nature* 397: 168–171. doi:10.1038/16483.
 26. Barkai N, Leibler S (1997) Robustness in simple biochemical networks. *Nature* 387: 913–917. doi:10.1038/43199.
 27. Hironaka K, Morishita Y (2014) Cellular Sensory Mechanisms for Detecting Specific Fold-Changes in Extracellular Cues. *Biophys J* 106: 279–288. doi:10.1016/j.bpj.2013.10.039.
 28. Tu Y, Shimizu TS, Berg HC (2008) Modeling the chemotactic response of *Escherichia coli* to time-varying stimuli. *Proc Natl Acad Sci* 105: 14855–14860. doi:10.1073/pnas.0807569105.
 29. Tu Y (2013) Quantitative modeling of bacterial chemotaxis: Signal amplification and accurate adaptation. *Annu Rev Biophys* 42: 337–359. doi:10.1146/annurev-biophys-083012-130358.
 30. Keller EF, Segel LA (1971) Model for chemotaxis. *J Theor Biol* 30: 225–234.
 31. Stryer L (1999) *Biochemistry*. W.H. Freeman. 1064 p.
 32. Whitford D (2005) *Proteins: structure and function*. John Wiley & Sons. Available: <http://www.google.com/books?hl=iw&lr=&id=qbHLkxbXY4YC&oi=fnd&pg=PR7&dq=Whitford,+David:+Proteins:+structure+and+function,+2005,+John+Wiley+%26+Sons&ots=c4FEIlgKd5u&sig=aWYtFIGAp5WW9jzBfMBfT0hs8>. Accessed 15 June 2014.
 33. Wartlick O, Mumcu P, Kicheva A, Bittig T, Seum C, et al. (2011) Dynamics of Dpp signaling and proliferation control. *Science* 331: 1154–1159.
 34. Wartlick O, Gonzalez-Gaitan M (2011) The missing link: implementation of morphogenetic growth control on the cellular and molecular level. *Curr Opin Genet Dev* 21: 690–695.
 35. Wartlick O, Mumcu P, Jülicher F, Gonzalez-Gaitan M (2011) Understanding morphogenetic growth control—lessons from flies. *Nat Rev Mol Cell Biol* 12: 594–604.
 36. Segel LA (1988) On the validity of the steady state assumption of enzyme kinetics. *Bull Math Biol* 50: 579–593.
 37. Glover DM, Jenkins WJ, Doney SC (2011) Least squares and regression techniques, goodness of fit and tests, and nonlinear least squares techniques. *Modeling Methods for Marine Science*. Cambridge University Press. Available: <http://dx.doi.org/10.1017/CBO9780511975721.004>.